Talanta 154 (2016) 312–321

Contents lists available at ScienceDirect

Talanta

journal homepage: www.elsevier.com/locate/talanta

Electrochemical DNA biosensor based on poly(2,6-pyridinedicarboxylic acid) modified glassy carbon electrode for the determination of anticancer drug gemcitabine

Gözde Aydoğdu Tığ [a,*], Bülent Zeybek [b], Şule Pekyardımcı [a]

[a] Ankara University, Faculty of Science, Department of Chemistry, Ankara 06100, Turkey
[b] Dumlupınar University, Faculty of Science and Arts, Department of Chemistry, Kütahya 43100, Turkey

ARTICLE INFO

Article history:
Received 27 December 2015
Received in revised form
11 March 2016
Accepted 15 March 2016
Available online 25 March 2016

Keywords:
Gemcitabine
dsDNA
Glassy carbon electrode
Polymer
Differential pulse voltammetry

ABSTRACT

In this study, a simple methodology was used to develop a new electrochemical DNA biosensor based on poly(2,6-pyridinedicarboxylic acid) (P(PDCA)) modified glassy carbon electrode (GCE). This modified electrode was used to monitor for the electrochemical interaction between the dsDNA and gemcitabine (GEM) for the first time. A decrease in oxidation signals of guanine after the interaction of the dsDNA with the GEM was used as an indicator for the selective determination of the GEM *via* differential pulse voltammetry (DPV). The guanine oxidation peak currents were linearly proportional to the concentrations of the GEM in the range of 1–30 mg L^{-1}. Limit of detection (LOD) and limit of quantification (LOQ) were found to be 0.276 mg L^{-1} and 0.922 mg L^{-1}, respectively. The reproducibility, repeatability, and applicability of the analysis to pharmaceutical dosage forms and human serum samples were also examined. In addition to DPV method, UV–vis and viscosity measurements were utilized to propose the interaction mechanism between the GEM and the dsDNA. The novel DNA biosensor could serve for sensitive, accurate and rapid determination of the GEM.

1. Introduction

Gemcitabine (GEM) is a cytosine nucleoside analog (Scheme 1) that is used as a chemotherapeutic agent in the treatment of a variety of solid tumors, such as pancreatic, lung, breast, bladder, brain and other types of cancers. GEM demonstrates good efficiency in combination with other cancer drugs [1, 2]. After intravenous (IV) administration, GEM undergoes metabolism by plasma and liver cytidine deaminase to form inactivated 2′,2′-difluorodeoxyuridine (dFdU) that is incorporated into DNA, which leads to apoptosis [3]. A rapid and sensitive analytical method for the detection of GEM is needed to provide alternative dosage and treatment procedures. Up until now, several chromatographic techniques, such as, HPLC [1,4] and LC/MS/MS [5,6], have been developed for the quantification of GEM in blood, urine, and tissues.

In recent years, considerable interest has been devoted to DNA biosensors to develop new techniques for the detection of many important molecules such as drugs [7–9] pathogens [10], and organic dyes [11,12]. Electrochemical DNA biosensors are constructed by immobilizing DNA on the electrode surface [13,14]. Electrochemical investigations of DNA and drug interactions have been significant a focus of interest in terms of their rapid, reliable and simple detection [15]. Direct monitoring of changes in the DNA's electrochemical properties, such as oxidation of guanine and adenine, allows the detection of the interaction of small molecules with DNA on the electrode surface [16,17].

The use of various polymers as electrode modifiers has recently become more popular in electrochemical biosensor applications [18,19]. These have been proposed as a suitable matrix for the adsorption of biomolecules and they can be used to enhance the stability, sensitivity and selectivity [20]. Electropolymerized 2,6-pyridinedicarboxylic acid (PDCA) film has been used in biosensor applications with different immobilized biomolecules due to its rich electroactive center, excellent stability, biocompatibility, and good infusible and insoluble capabilities [21,22]. Studies have shown that electropolymerization of PDCA can provide a suitable surface for the immobilization of DNA [21,23].

Kalanur et al. reported the interaction of GEM with dsDNA in a phosphate buffer solution (PBS) (pH 7.4) at a glassy carbon electrode (GCE) and the analytical application of the assay for GEM [24]. In this study, one peak corresponding to the oxidation of GEM was observed at 0.927 V (*vs.* Ag/AgCl). The electrochemical

* Corresponding author.
E-mail address: gaydogdu@science.ankara.edu.tr (G.A. Tığ).

http://dx.doi.org/10.1016/j.talanta.2016.03.049
0039-9140/

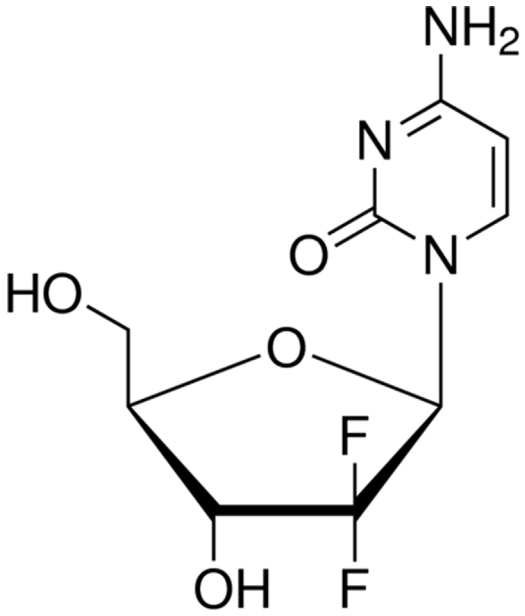

Scheme 1. The chemical structure of gemcitabine.

analysis of GEM and the interaction mechanism between the dsDNA and the GEM were explained using this peak. Florea et al. reported a different technique based on a molecularly imprinted polymer sensor. They investigated the changes in the reduction peak of $[Fe(CN)_6]^{3-/4-}$, which is a mediator for the detection of GEM [25]. In another study, Buoro et al. investigated the interaction between GEM and DNA using a DNA-electrochemical biosensor [26]. No electrochemical process related to the oxidation or reduction of GEM was observed at the GCE in the potential range between −0.70 and +1.40 V (*vs.* Ag/AgCl) in various electrolytes, such as PBS and acetate buffer solution (ABS). Similar to this study, we did not observe any peaks for the oxidation of GEM in ABS (pH 4.8). Therefore, the experimental studies in this paper were constructed based on the changes of the guanine base in the DNA.

In this study, a simple poly(2,6-pyridinedicarboxylic acid) modified glassy carbon electrode (GCE/P(PDCA)) was prepared, and then the GCE/P(PDCA) was activated by a pre-treatment procedure to provide a positive charge density on the polymer surface. The dsDNA was immobilized on the surface of the GCE/P (PDCA) *via* an adsorption technique in ABS (pH 4.8). The developed DNA biosensor was employed for the electrochemical determination of GEM for the first time. This sensitive and selective electrochemical DNA biosensor showed wide linear range and low detection limit for the determination of GEM, which was performed based on the changes in the guanine signal. Moreover, the interaction mechanism between the dsDNA and GEM was examined by DPV, UV–vis spectroscopy, and viscosity measurement techniques. The proposed DNA biosensor was successfully applied for the determination of GEM in pharmaceutical formulations and human serum samples.

2. Experimental

2.1. Chemicals

Fish sperm dsDNA was purchased from Serva Electrophoresis GmbH Co. (Germany). GEM, PDCA, sodium acetate, sodium chloride, and acetic acid were provided by Sigma Chemical Co., Ltd. Gemful® 1000 mg, for infusion, was purchased from a local pharmacy. 1.0 mg/mL of dsDNA stock solution was prepared in ultrapure water and stored at −20 °C. Solutions of different concentrations of dsDNA and GEM were prepared by dilution in 0.5 mmol L^{-1} ABS (pH 4.8). Solutions of 1 mg/mL GEM were prepared daily using ultrapure water. Other chemicals were analytical grade and used without further purification.

2.2. Apparatus

Electrochemical measurements were performed with an Autolab PGSTAT 302N potentiostat/galvanostat measurement system using Nova 11.1 software (Eco Chemie, The Netherlands). The experiments were conducted in a voltammetric cell Bioanalytical Systems, Inc., USA using a conventional three-electrode system. Silver/silver chloride (BAS MF2052), platinum wire (BAS MF1032), and bare or GCE/P(PDCA) electrodes were used as the reference, counter and working electrodes, respectively. The pH measurements were obtained using an ORION Model 720A pH meter (Thermo Scientific USA). The ultrapure water (18.2 MΩ cm) from Purelab Elga system (Veolia Water Systems Ltd., UK) was employed for preparing all solutions. All measurements were carried out at room temperature.

Electrochemical characterizations of GCE/P(PDCA) and GCE/P (PDCA)/dsDNA were achieved in a 0.1 mol L^{-1} KCl solution including 5.0 mmol L^{-1} $Fe(CN)_6^{3-/4-}$ by cyclic voltammetry (CV) and electrochemical impedance spectroscopy (EIS) techniques. The cyclic voltammograms (CVs) were obtained by scanning in the potential window from −0.3 to 0.6 V at a scan rate of 50 mV s^{-1}. For the impedance measurements, a frequency range of 100–0.01 Hz was used with an AC voltage amplitude of 5 mV at an open-circuit potential (E_{OCP}).

The Fourier transform infrared (FT-IR) spectra of the powder PDCA and P(PDCA) film on the surface of the GCE were carried out directly using a Bruker Alpha spectrometer connected to an ATR attachment (Bruker Corporation Ltd.) in the range of 650–2000 cm^{-1} with a spectral resolution of 4 cm^{-1}. The spectrum of the P(PDCA) film coated GCE was measured by placing the electrode onto the DRIFT module. The modified electrodes were characterized by a scanning electron microscopy (FEI Nova NanoSEM 650, The Netherlands).

X-Ray photoelectron spectroscopy (XPS) analyses were performed using a PHI 5000 Versa Probe spectrophotometer equipped with an Al KαX-ray source (1486.6 eV) at an incident angle of 45°. The pass energy for XPS was 20 eV. The C 1s and N 1s XPS spectra were measured at 0.1 eV step size. Multiplex scan fitting was accomplished with Gaussian–Lorentzian functions.

UV–vis absorption spectra were obtained with a Shimadzu 1700 (Pharma Spec) double beam spectrophotometer (Shimadzu Corporation, Tokyo, Japan) using quartz cuvettes of 1 cm path length at room temperature in the wavelength range of 200–500 nm. The spectra were recorded for free dsDNA and dsDNA-GEM for the calculation of the binding constant of the reaction occurring between the GEM and the dsDNA.

Viscosity experiments were performed using an Ubbelohde viscometer at 25 ± 0.1 °C in a thermostatic water-bath. GEM concentrations ranging from 0 to 30 mg L^{-1} were added to the viscometer to give a certain molar ratio of GEM to dsDNA, and the concentration of dsDNA was fixed at 30 mg L^{-1}. After each addition of GEM, the solution was allowed to reach the thermal equilibrium by waiting for 60 min, and then the flow time of the sample through the capillary was measured using a digital chronometer. The relative viscosity values of the dsDNA in the absence and presence of GEM were calculated from the following equation:

$$\frac{\eta}{\eta_0} = \frac{(t - t_0)}{(t_{dsDNA} - t_0)}$$

where t_0 and t_{dsDNA} are the flow time of the 0.5 mol L^{-1} ABS containing 20 mmol L^{-1} NaCl and dsDNA, respectively, while t is the flow time of the GEM and dsDNA mixture. The data have been presented as $(\eta/\eta_0)^{1/3}$ plotted *versus* the [GEM]/[dsDNA] ratio, where η refers to the relative viscosity of the dsDNA after the addition of GEM and η_0 denotes the relative viscosity of dsDNA alone.

2.3. Electrochemical synthesis of P(PDCA) film

The surface of the GC electrode was polished using a polishing microcloth with 0.05 μm alumina powder and then rinsed several times with ultrapure water, sonicated in water and then the electrode was dried at room temperature. A freshly prepared solution (10 mL) containing 0.1 mol L^{-1} KCl and 1.0 mmol L^{-1} 2,6-pyridinedicarboxylic was degassed with free nitrogen to remove oxygen. A series of eighteen potential sweeps were applied between 0.0 V and +2.0 V at a scan rate of 60 mV s^{-1} [22]. The obtained CVs (Fig. S1) are given in the Supplementary material. After this procedure, the GCE was covered with a thin film of P (PDCA), and this electrode was washed with ultrapure water. Yang et al. [22] and Kui et al. [27] reported that the surface of the P (PDCA) polymer film synthesized under these conditions had a negative charge and repelled substances with a negative charge such as $Fe(CN)_6^{3-/4-}$. A pre-treatment or activation procedure for the polymer film was required to accomplish immobilization of the negatively charged dsDNA. For this purpose, the polymer was activated by applying ten successive differential pulse voltammograms (DPVs) in the potential range from +0.4 to +1.3 V (*vs.* Ag/AgCl) in 0.1 mol L^{-1} ABS (pH 4.8). The cyclic voltammogram and EIS spectrum (Nyquist plot) of GCEs modified with both untreated and pre-treated P(PDCA) were recorded in the solutions containing 5.0 mmol L^{-1} $Fe(CN)_6^{3-/4-}$ as a redox probe, and they are shown in the Supplementary material (Figs. S2 and S3). Unless otherwise stated, the pre-treated polymer film was used in the experimental studies.

2.4. Adsorption of dsDNA onto polymeric film

For the adsorption of the dsDNA, the modified electrodes were immersed into vials containing 40 mg L^{-1} dsDNA in 0.5 mol L^{-1} acetate buffer solution (0.02 mol L^{-1} NaCl) for 30 min. After adsorption of the DNA, the electrode was washed with acetate buffer (0.5 mol L^{-1} at pH 4.8) for 5 s.

2.5. Interaction of dsDNA with GEM

To investigate the interaction between the GEM and the dsDNA on the P(PDCA) film modified GCE, the guanine oxidation signal was used as an indicator. After the adsorption of dsDNA onto GCE/P(PDCA), it was immersed into in 0.5 mol L^{-1} acetate buffer (pH 4.8) solution containing different concentration of GEM and stirred at 200 rpm for selected times. After the interaction, the electrode was rinsed and placed in GEM-free acetate buffer solution, where the DPV was recorded.

The DPVs were obtained in 0.5 mol L^{-1} pH 4.8 acetate buffer solution by scanning in the potential range from +0.4 to +1.3 V. The experimental conditions for the differential pulse voltammetry were step potential: 0.003 V; modulation amplitude: 0.05 V; modulation time: 0.02 s; interval time: 0.2 s and scan rate: 0.015 V s^{-1}. The anodic current was +0.8 V, which corresponds to the guanine oxidation, and it was employed as an analytical signal.

2.6. Preparation of real samples

Commercial pharmaceutical formulation samples of Gemful® (1000 mg) were selected for the analysis of the GEM. Adequate amounts of Gemful® were dissolved in 10 mL ultrapure water. An aliquot of the sample solution was transferred into a volumetric vial and diluted with ABS. The GEM content was determined according to the recommended procedure.

Human serum samples supplied from healthy individuals were selected and stored at −20 °C until the assay procedure. After a 10 μL volume of serum was transferred into vial containing 90 μL acetate buffer solution, a certain volume of the stock solution of GEM was added into the vial. This mixture was transferred to an electrochemical cell, and left to interact with the GCE/P(PDCA)/dsDNA electrode for the selected time. After the interaction, the GCE/P(PDCA)/dsDNA electrode was rinsed and placed in blank ABS and the DPVs were recorded.

3. Results and discussion

3.1. FT-IR spectrum of P(PDCA) film

To demonstrate the formation of the P(PDCA) film on the surface of the GCE, the FT-IR spectroscopy technique was utilized. The FT-IR spectra of the PDCA monomer and P(PDCA) film were recorded and are given in Fig. S4. As seen from the figure, there were apparent differences between the monomer and polymer spectra and this finding supports the presence of a polymer film on the electrode surface. The main IR bands and their positions are shown in Table S1. In the spectrum of P(PDCA), the characteristic bands between 1728 and 1644 cm^{-1} were assigned to the stretching vibration of the C=O group [28]. The band observed at 1611 cm^{-1} was attributed to the C=C/C–C and C–N/C=N stretching vibrations of the pyridine ring [29–31]. The band at approximately 1553 cm^{-1} may be ascribed to the C=C, C=N and asymmetric COO^- stretching vibrations in the PDCA unit [32,33]. The band observed at 1450 cm^{-1} can be assigned to the O–H in-plane bending vibrations in the PDCA unit [34] and/or the symmetric COO^- vibration [28]. The band appearing at 1385 cm^{-1} may be concerned to the symmetric COO^- stretching vibrations and the O–H in-plane bending vibrations in the PDCA unit [30,32]. The bands at 1297 and 1219 cm^{-1} may be related to the C–O and C–N stretching vibrations, respectively. The O–H and C–H in-plane bending vibrations and stretching vibrations of the pyridine ring were observed at 1157 cm^{-1}. The bands at around 991, 901, 878 and 753 cm^{-1} pertained to the O–H and C–H out-of-plane bending vibrations in the PDCA unit [30, 31, 34]. The in-plane bending vibrations of $(O–C–O)^-$ appeared at 691 cm^{-1} [35]. The broadening of the spectrum of the polymer and decrease in the number of peaks when compared to the monomer demonstrated that the P(PDCA) was coated onto the GCE surface.

3.2. SEM images of P(PDCA) modified electrodes

The surface morphologies of the bare GCE, GCE/P(PDCA) and GCE/P(PDCA)/dsDNA were investigated using SEM. Fig. 1(a) displays the SEM image of the bare GCE and this electrode had a uniform and smooth structure. When the surface of GCE modified with the P (PDCA), a homogeneous thin film occurred on the electrode surface and its surface morphology changed (Fig. 1(b), (c)). As seen in Fig. 1 (d), (e), a heterogeneous layer on the polymer surface was observed after immobilization of dsDNA. The dsDNA agglomerated to the surface more densely in certain regions. To further confirm the formation of polymer film on the electrode surface and immobilization of dsDNA on polymer film, the energy dispersive X-ray spectroscopy (EDS) analyses were conducted and the spectra were shown in Fig. 1(f) and (g). The existence of P(PDCA) on GCE surface was seen from the peaks of C, O and N elements in EDS data (Fig. 1 (f)). The incorporation of ionic chloride species as dopant into polymer backbone was proved by the Cl signal. In the case of GCE/P

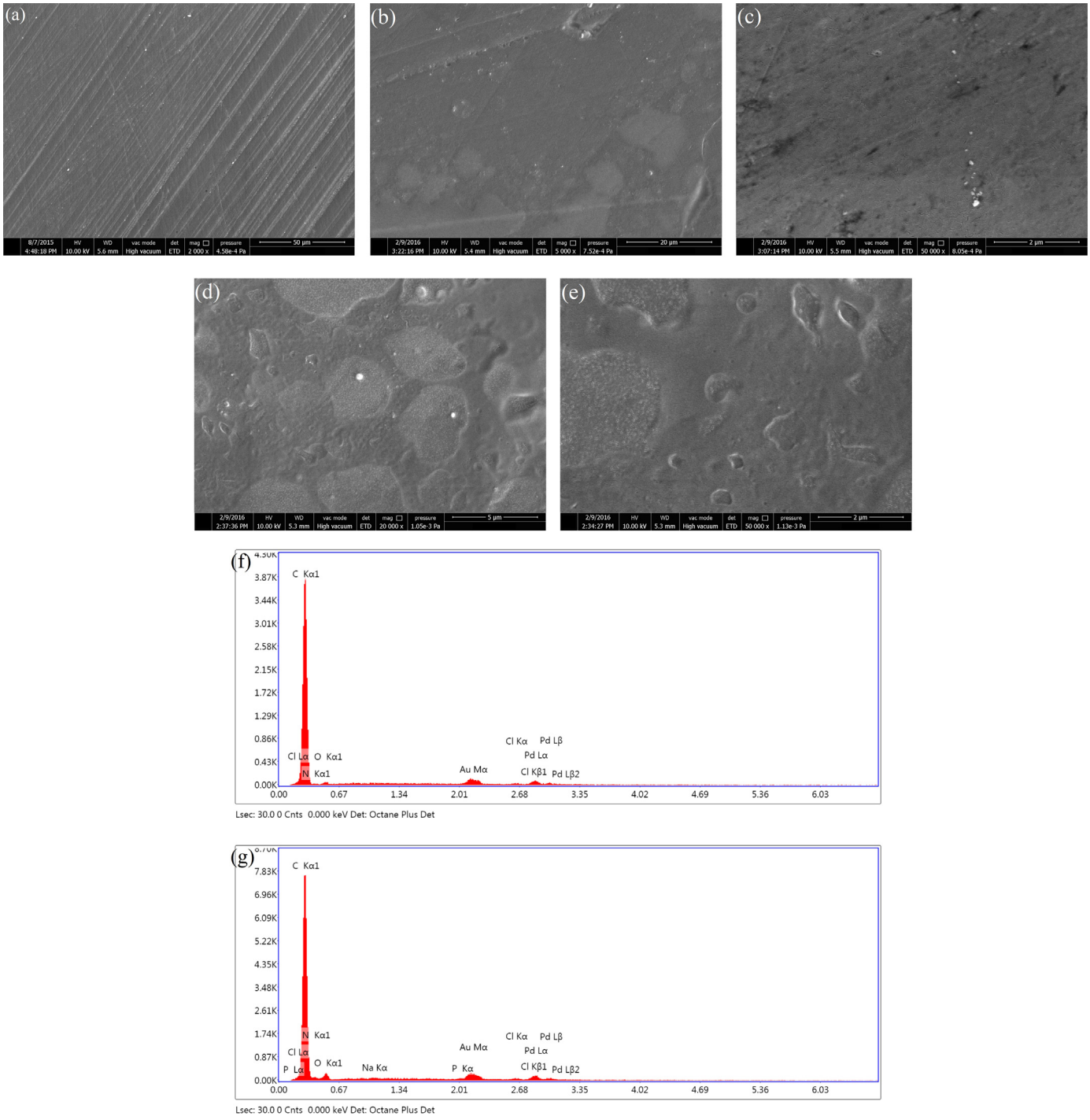

Fig. 1. SEM images of bare GCE (a), GCE/P(PDCA) (b,c), GCE/P(PDCA)/dsDNA (d,e), the EDS spectra of P(PDCA) film (f) and GCE/P(PDCA)/dsDNA (g).

(PDCA)/dsDNA, the P signal was also observed in EDS data (Fig. 1 (g)). This confirms the successfully immobilization of dsDNA upon the surface of the GCE/P(PDCA).

3.3. X-ray photoelectron spectroscopy (XPS)

To demonstrate presence of P(PDCA) polymer film and dsDNA on the GCE surface, XPS measurements were also performed. Fig. 2 shows survey spectra of bare GCE (a), GCE/P(PDCA) (b) and GCE/P (PDCA)/dsDNA (c) when the dsDNA adsorption reached 40 mg L^{-1}. The presence of a O1s peak on the bare GCE may be due to the effect of surface oxidation and surface preparation procedure [36]. The XPS spectrum shown in Fig. 2(b) clearly reveals that the Cl 2p (198.7 eV), Cl 2s (270.2 eV), C1s (285.0 eV), N 1s (400.6 eV) and O 1s (532.2 eV) are present at the surface of GCE/P(PDCA). The appearance of the N 1s and Cl 2p signals as well as decreasing of the percentage of C 1s signal indicates the presence of P(PDCA) on the GCE surface. After the adsorption of the dsDNA, the XPS spectra of the GCE/P(PDCA)/dsDNA electrode exhibited new P 2p, P 2s, NaKLL, and Na 1s signals at about 133.2, 198.0, 495.0, and 1072.0 eV, respectively (Fig. 2(c)). This verifies that the dsDNA was immobilized on the GCE/P(PDCA) surface.

In the expanded XPS spectra, the C 1s peaks at 283.0, 284.2, 286.5, and 290.7 eV shown in Fig. S5(A) can be assigned to carbon

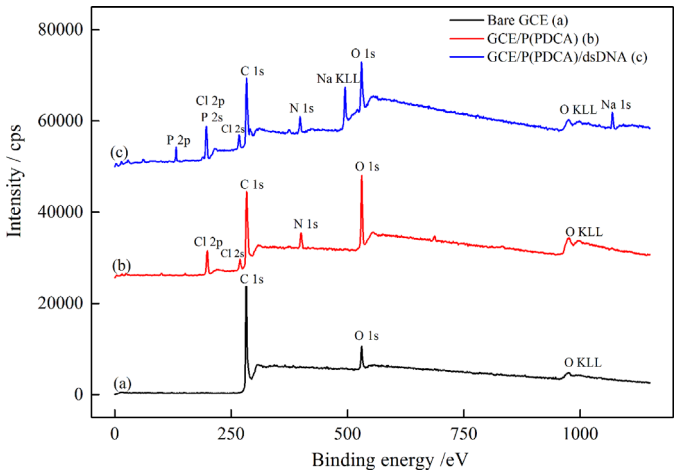

Fig. 2. XPS survey spectra of (a) bare GCE, (b) GCE/P(PDCA) and (c) GCE/P(PDCA)/dsDNA electrode.

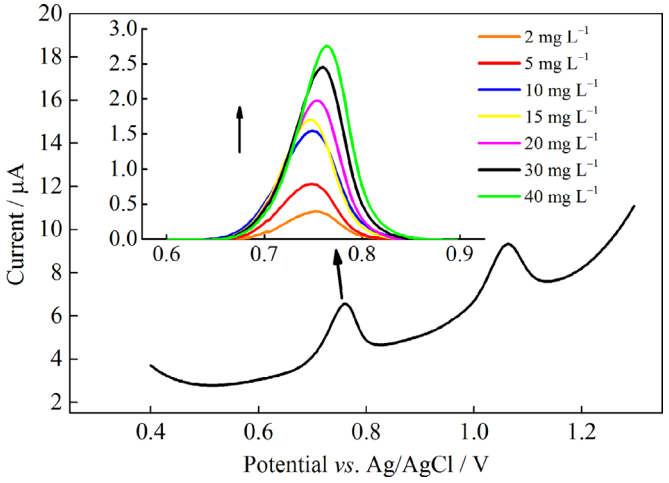

Fig. 3. Differential pulse voltammogram of the GCE/P(PDCA) electrode adsorbed the 30 mg L^{-1} dsDNA (inset: the oxidation peaks of guanine at dsDNA amounts varying from 2 mg L^{-1} to 40 mg L^{-1}).

in the form of C–C, C–N, C=O, and O–C=O, respectively [37,38]. The N 1s peaks at 398.1 and 400.7 eV shown in Fig. S5(B) are associated with nitrogen in the states of C=N and C–N, respectively [39].

3.4. Electrochemical characterizations of bare GCE, GCE/P(PDCA) and GCE/P(PDCA)/dsDNA

CV and EIS techniques were employed for the electrochemical characterizations of the bare GCE, GCE/P(PDCA) and GCE/P(PDCA)/dsDNA electrodes in 0.1 mol L^{-1} KCl containing 5.0 mmol L^{-1} $Fe(CN)_6^{3-/4-}$. Fig. S6(A) illustrates the CVs of the bare and modified GCEs at a scan rate of 50 mV s^{-1}. When the surface of the GCE was coated with P(PDCA), a decrease in the peak to peak separation (ΔE_p) and an increase in the anodic and cathodic peak currents were observed, which might be ascribed to the electrostatic attraction of the positively charged P(PDCA) to $Fe(CN)_6^{3-/4-}$ ions. In the case of the GCE/P(PDCA)/dsDNA electrode (Fig. S6(A) (c)), a decrease in the peak currents of the redox probe and an increase in the ΔE_p were observed according to the P(PDCA) modified electrode. The results indicated that the negatively charged dsDNA had been adsorbed on the surface of the GCE/P(PDCA), and this impedes the $Fe(CN)_6^{3-/4-}$ ions access to the surface of the GCE [40].

To obtain more information about the electron transfer kinetics, the EIS technique was also used. A semicircle part at high frequencies and a linear part at low frequencies occur in a typical an EIS spectrum (Nyquist plot). The semicircle part and the linear part correspond to the electron transfer limited process and the diffusion process, respectively. The semicircle diameter is equal to electron transfer resistance (R_{et}) value. Fig. S6(B) shows the Nyquist plots for the bare GCE (a), GCE/P(PDCA) (b), and GCE/P(PDCA)/dsDNA (c). When the surface of the GCE was coated with P(PDCA), the R_{et} value of the P(PDCA) modified GCE was smaller than that of the bare GCE. When compared with the GCE/P(PDCA) electrode, the R_{et} value of the GCE/P(PDCA)/dsDNA electrode increased due to the adsorption of the DNA onto the surface of the P(PDCA) film [22]. The impedance results were in good agreement with the CVs performed under the same conditions (Fig. S6(A)).

3.5. Adsorption of dsDNA onto GCE/P(PDCA) electrode

The immobilization of the dsDNA on the surface of the GCE/P(PDCA) electrode was performed by the direct adsorption method. Fig. 3 shows the DPVs of the GCE/P(PDCA)/dsDNA electrodes in the dsDNA concentration range of 5–40 mg L^{-1}. The guanine oxidation peak currents increased with increasing dsDNA concentration until 40 mg L^{-1} and then leveled off (Fig. 4(A)). Thus, the optimum dsDNA concentration was selected as 40 mg L^{-1}. One important parameter for the immobilization of dsDNA is the adsorption time. Fig. 4(B) presents the guanine oxidation signals at the GCE/P(PDCA)/dsDNA for 40 mg L^{-1} of dsDNA at different accumulation periods. The DPV signals of guanine increased up to 30 min of the adsorption time and then leveled off. Therefore, 30 min was chosen as the optimum adsorption time of the dsDNA for the preparation of the GCE/P(PDCA)/dsDNA.

3.6. Electrochemical studies for the interaction of GEM with dsDNA at GCE/P(PDCA)

The effects of the interaction time and concentration of GEM were investigated to determine the optimum conditions for the interaction between the GEM and the dsDNA. Firstly, the interaction time between GEM and dsDNA at the GCE/P(PDCA) was optimized. As shown in Fig. 5(A), after the interaction with GEM, there was a decrease in the guanine oxidation signal till 150 s, and then it almost leveled off completely between 150 and 180 s. Accordingly 150 s was considered to be the optimum time for the interaction between GEM and dsDNA. Secondly, the effect of the concentration of the GEM on the DPV signals in the presence of 40 mg L^{-1} dsDNA was evaluated in the concentration range of 0 and 40 mg L^{-1}. Fig. S7 shows the DPVs of the dsDNA at the GCE/P(PDCA) electrode for the various concentration of GEM (Supplementary material). Increasing the concentration of the GEM caused a decrease in the oxidation peak current for the guanine and adenine. The decrease in the guanine oxidation peak currents may be attributed to the binding of the GEM to the dsDNA. This decrease could be explained as a possible damage in the oxidizable groups of the electroactive bases of DNA while GEM interacts with the dsDNA at the GCE/P(PDCA) surface [41,42]. Generally, the positive shifts or negative shifts in the oxidation peak potential of guanine showed the binding form to be *via* intercalation or electrostatic binding, respectively [43]. Since Fig. S7 clearly indicate no measurable shift in the oxidation peak potential of guanine of upon addition of GEM, it can be concluded that the binding mode of the GEM to the dsDNA is neither electrostatic interaction nor intercalative binding. As shown in Fig. 5(B), the oxidation peak currents of guanine were linear with the GEM concentration over the range of 1.0–30.0 mg L^{-1} with a linear equation of $I(\mu A) = -$

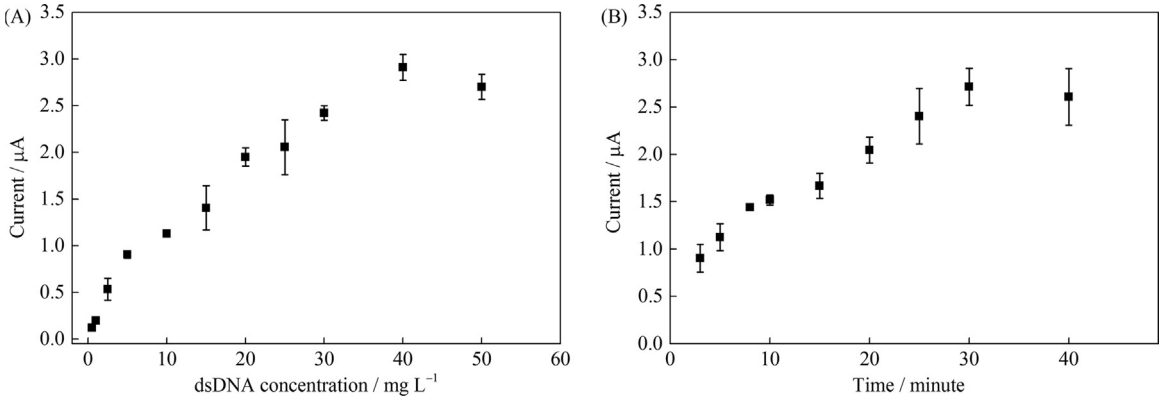

Fig. 4. The effect of dsDNA concentration (A) and adsorption time (B) on the electrochemical responses of guanine at GCE/P(PDCA)/dsDNA.

$0.0217C+1.368$ with $R^2=0.991$ ($n=3$) where C is the GEM concentration in mg L^{-1}. The limit of detection (LOD) and limit of quantification (LOQ) from the calibration curve were found to be 0.276 and 0.922 mg L^{-1}, respectively. The LOD and LOQ values confirmed the sensitivity of the modified electrode which was calculated using the following equation [14].

$$\mathrm{LOD} = 3\ s/m,\ \ \mathrm{LOQ} = 10\ s/m \quad (1)$$

where s is the standard deviation of the current (three runs) for the lowest concentration of the linearity range, m is the slope of the related calibration curve. The analytical parameters obtained for the GEM determination using the DPV method are shown in Table 1. To evaluate the precision of the suggested method, repeatability and reproducibility studies were performed (Table 1). The repeatability of the dsDNA adsorbed modified electrode was evaluated by measuring the guanine oxidation signal at the same electrode. The relative standard deviation (RSD) of the five repeated measurements was 3.51%. The reproducibility of the GCE/P(PDCA)/dsDNA was calculated from the changes in the oxidation peak current for the guanine signal obtained by five different electrodes. (Table 1). The RSD value of reproducibility was found to be 3.72%. As shown in Table 2, the proposed GCE/P(PDCA)/dsDNA electrode shows comparable analytical performance with the reported methods [24–26,44,45].

There are three modes of binding for small molecules, such as drugs, to dsDNA. These interactions involve intercalation, electrostatic interaction, and groove binding [46]. Among them, electrostatic interaction happens out of the groove of the dsDNA. In contrast, the intercalation and groove binding modes occur on the DNA double helix. Differential pulse voltammetry was utilized to study the interaction of the dsDNA with the GEM, because this technique can provide some information to determine the mode of interaction. Furthermore, the DPV can reduce the background effects when studying the electrochemical behavior of biological systems. If there is a negative or positive shift in the oxidation peak potential, this can be considered to be an electrostatic or intercalative interaction, respectively [43]. As shown in Fig. S7, a notable shift in the peak potential of the guanine and adenine signals upon the addition of the GEM was not observed. Furthermore, the decrease in the peak current of the dsDNA with the addition of the GEM was due to the decrease in the equilibrium concentration of the free dsDNA. It can be assumed that a GEM-dsDNA complex (Eq. (2)) occurred between the dsDNA and GEM, and that this complex was electrochemically more inactive than

Table 1
Analytical characteristics for voltammetric determination of GEM using DPV at GCE/P(PDCA)/dsDNA electrode.

Parameters	Obtained results
Potential applied (V)	0.78
Linearity range (mg L^{-1})	1–30
Sensitivity (μA mg^{-1} L)	−0.0217
Determination coefficient (R^2)	0.991
SE of slope	8.4×10^{-4}
SE of intercept	0.0142
LOD (mg L^{-1})	0.276
LOQ (mg L^{-1})	0.922
RSD for repeatability[a]	3.51%
RSD for reproducibility[a]	3.72%

[a] Each value is the mean of the three measurements.

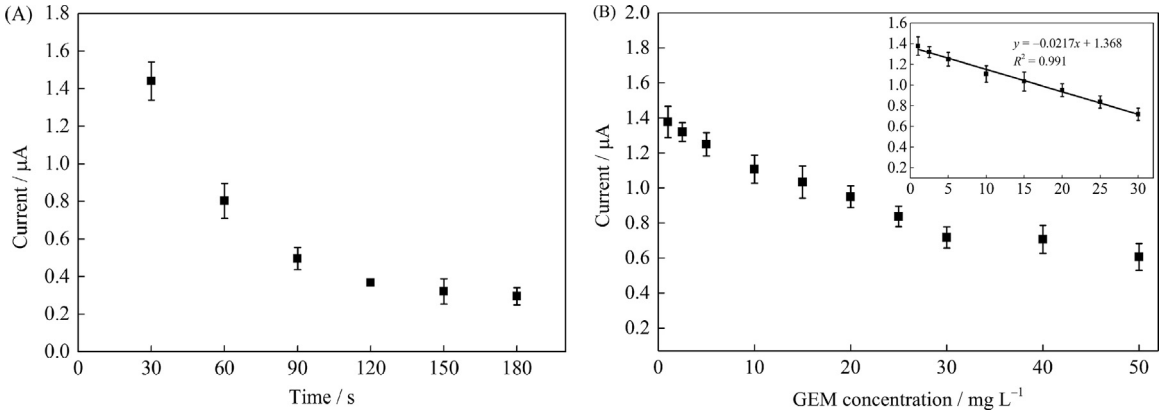

Fig. 5. (A) The effect of the interaction time and (B) concentration of GEM with dsDNA on the guanine oxidation peak current (inset: linear dependence of GEM concentration on the guanine signals at GCE/P(PDCA)/dsDNA electrode) (0.5 mmol L^{-1} ABS, pH 4.8).

Table 2
Comparison of analytical performances of the different electrochemical sensors for the determination of GEM.

Electrode	Linearity	LOD	Repeatability	Application	References
GCE	5 μmol L^{-1} to 0.75 mmol L^{-1}	1.06 μmol L^{-1}	RSD: 1.68%	Injection solution Recoveries: 96.53–98.83	[24]
MIP/AuE	3.8 fmol L^{-1} to 38 nmol L^{-1}	3.0 fmol L^{-1}	RSD: 5.5% (n=3)	Serum Recoveries: 96.38–102.03	[25]
GCE/dsDNA	nr	nr	nr	nr	[26]
AuE	0.1–15.0 μmol L^{-1}	0.06 μmol L^{-1}	RSD: 1.31% (n=6)	Urine Recoveries: 98.29–102.55%	[44]
CPE	5.0×10^{-8}–3.0×10^{-4} mol L^{-1}	8.2×10^{-9} mol L^{-1}	RSD: 2.53% (n=6)	Urine Recoveries: 98.02–99.70	[45]
GCE/P(PDCA)/dsDNA	3.8–114 μmol L^{-1}	1.0 μmol L^{-1}	RSD: 3.51% (n=5)	Injection solution Recoveries: 101.6–106.0	This study

Glassy carbon electrode (GCE), molecularly imprinted polymer (MIP), gold electrode (AuE), double stranded DNA (dsDNA), carbon paste electrode (CPE), poly(2,6-pyridinedicarboxylic acid) (P(PDCA)), relative standard deviation (RSD), not reported (nr).

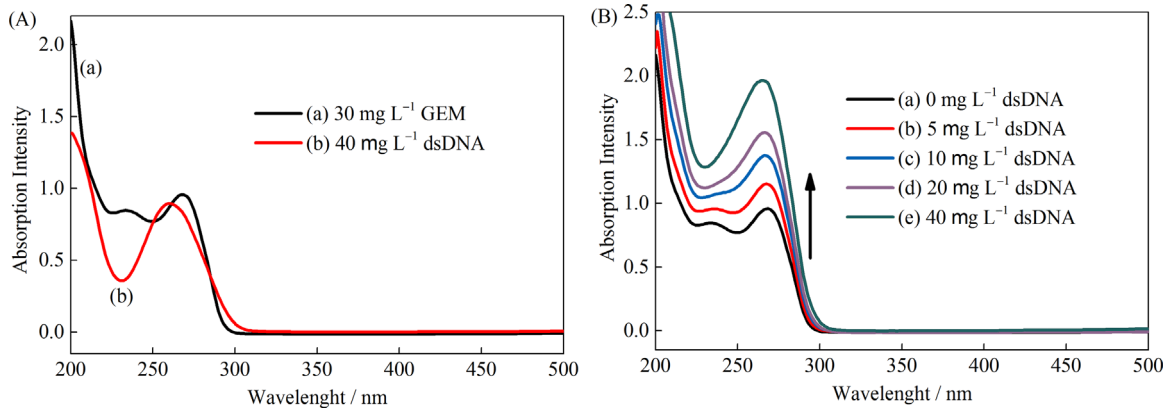

Fig. 6. UV–vis spectra of (A) GEM (30 mg L^{-1}) and dsDNA (40 mg L^{-1}), (B) GEM (30 mg L^{-1}) in the absence and presence of dsDNA in the range of 5–40 mg L^{-1}.

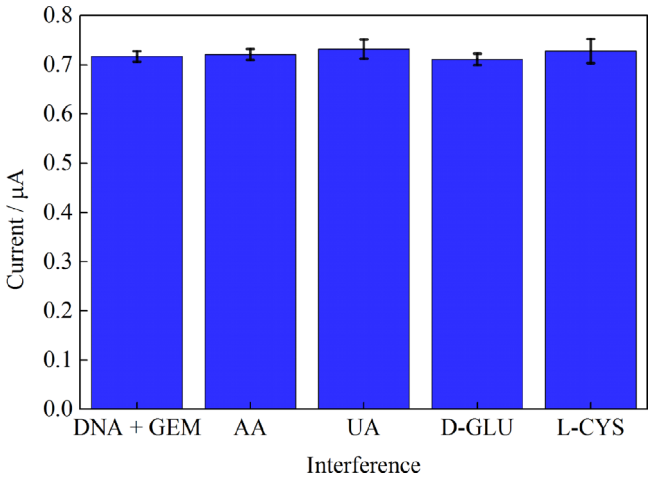

Fig. 7. DPV peak currents of GCE/P(PDCA)/dsDNA for 30 mg L^{-1} GEM in 0.5 mmol L^{-1} ABS (pH 4.8) containing 0.02 mmol L^{-1} NaCl before (dsDNA+GEM) and after adding of 0.01 mmol L^{-1} ascorbic acid (AA), uric acid (UA), D-glucose (D-GLU), and L-cysteine (L-CYS).

the dsDNA.

$$\text{dsDNA} + \text{GEM} \rightleftharpoons \text{GEM} - ds\text{DNA} \quad (2)$$

Table 4
Determination of GEM in serum samples.

Sample no.	Amount of added (mg L^{-1})	Amount of found (mg L^{-1})	Recovery (%)	RSD[a] (%)	Bias (%)
1	1.00	1.002	100.20	3.12	0.20
2	10.00	10.08	100.80	2.36	0.80
3	20.00	20.60	103.00	1.03	3.00

[a] Each value is the mean of three measurements

If it is supposed that the interaction of the GEM with the dsDNA generates only one complex, the interaction between GEM and dsDNA can be determined by using the following equation [47,48]:

$$\log\left(\frac{1}{[\text{GEM}]}\right) = \log K + \log\left(\frac{I_{\text{GEM-dsDNA}}}{I_{\text{ds DNA}} - I_{\text{GEM-dsDNA}}}\right) \quad (3)$$

where K is the binding constant, I_{dsDNA} is the peak current of the dsDNA and $I_{\text{GEM–dsDNA}}$ is the peak current of the GEM–DNA complex formation after the interaction of the drug with the DNA that is immobilized on the surface of the electrode. The binding constant value of this complex, K, can be determined from the intercept of the non-linear curve fitting plot of log(1/[GEM]) *vs.* log ($I_{\text{GEM–dsDNA}}/I_{\text{dsDNA}} - I_{\text{GEM–DNA}}$). The value of K is calculated as 4.6×10^4 L mol^{-1}.

Table 3
Recovery of gemcitabine in commercial injection formulations.

Labeled claim (mg L^{-1})	Amount of found (mg L^{-1})	Amount of added (mg L^{-1})	Amount of found (mg L^{-1})	Recovery (%)	RSD[a] (%)	Bias (%)
1.00	1.03	1.00	0.98	98.00	4.58	−2.0
5.00	5.02	5.00	4.98	99.60	2.18	−0.4
10.00	10.08	10.00	9.78	97.80	3.08	−2.2

[a] Each value is the mean of three measurements

3.7. UV–visible absorption studies

Absorption spectrophotometry was used to clarify the interaction between GEM and the dsDNA. The UV–visible absorption spectra of the dsDNA and the dsDNA-GEM system were measured in ABS (pH 4.8). The GEM presented two absorption peaks at about 237 and 269 nm which were close to the absorption peak of dsDNA at 260 nm (Fig. 6(A)). With the addition of dsDNA (5–40 mg L^{-1}) to the fixed concentration of GEM (30 mg L^{-1}), an increase in the absorption spectrum of the GEM at 269 nm (hyperchromism) with a slight blue shift was observed (Fig. 6(B)). The results indicated that there is an interaction between the dsDNA and the GEM. In addition, the total absorption intensities of the free dsDNA and free GEM were lower than those of the dsDNA-GEM complexes (Table S2). Generally, it is accepted that the binding of small molecules to dsDNA through intercalation usually results in hyperchromism and significant red shift ($\geq$ 15 nm), while outside binders show a smaller red shift ($\leq$ 8 nm) [24,49]. In the case of groove binding molecules, which bind on the outer surface of the DNA, smaller or no bathochromism is usually observed [50]. The UV spectrum results of the GEM-DNA complex suggest that GEM may interact with dsDNA *via* groove binding. Based upon the variations in the absorbance spectra of GEM upon binding to the dsDNA, the binding constant (K) can be determined according to following equation:

$$\frac{A_0}{A - A_0} = \frac{\varepsilon_G}{\varepsilon_{H-G} - \varepsilon_G} + \frac{\varepsilon_G}{\varepsilon_{H-G} - \varepsilon_G} \times \frac{1}{K\,[\mathrm{DNA}]} \quad (4)$$

where K is the binding constant and, A_0 and A are the absorbance values of the drug and its complex with dsDNA, respectively. ε_G and ε_{H-G} are the absorption coefficients of the drug and the GEM–dsDNA complex, respectively. The binding constant, K, can be obtained from the intercept-to-slope ratio of $A_0/(A–A_0)$ *vs.* 1/[dsDNA] plot. The value of K for GEM–dsDNA interaction was calculated to be 3.4×10^4 L mol^{-1}. Moreover, it was close to the value obtained from the DPV method (4.6×10^4 L mol^{-1}). It can be concluded that the interaction type between the dsDNA and GEM may be the groove binding mode [24].

3.8. Viscosity studies

A useful technique to determine the binding mode between small molecules and DNA is viscosity measurement, which is sensitive to the length change of the double helix, and it is the most critical test of the classical intercalative binding mode. Generally, a classical intercalative binding of small molecules causes an increase in the viscosity of the DNA solution. Conversely, non-intercalation binding, such as electrostatic or groove binding, may have little impact on the viscosity of DNA since they do not alter the axial length of the dsDNA upon binding [51–53]. As seen in Fig. S8, the relative viscosity of the dsDNA showed a trivial change that indicated the binding mode of GEM with dsDNA was not an intercalative interaction. Such behavior suggests further that a non-intercalative, and possibly a groove, binding should be the interaction mode of GEM with dsDNA.

3.9. Effect of NaCl concentration

An investigation of the effect of the salt concentration provides useful information to understand the binding mode between small molecules and dsDNA. To clarify the interaction of the GEM (30 mg L^{-1}) with the dsDNA (40 mg L^{-1}) adsorbed at the GCE/P(PDCA) surface, the effect of ionic strength on the guanine oxidation signal was investigated. DPVs were obtained in 0.5 mmol L^{-1} ABS (pH 4.8) containing different concentrations of NaCl (2.5–30 mmol L^{-1}) (Fig. S9). The electrostatic attraction between the small molecule and the dsDNA usually serves as an auxiliary mode to assist intercalation and groove binding. If the electrostatic interaction takes place between the binding of small molecules and dsDNA, the strength of the interaction decreases with an increase in the salt concentration in the solution [51,54]. The obtained data showed that the peak current of guanine almost did not change with the increase in the concentration of NaCl, which indicated that there was no significant electrostatic binding between the GEM and dsDNA.

3.10. Interference study

Interference studies were performed at the GCE/P(PDCA)/dsDNA with several interfering compounds prior to the application of the developed biosensor for the analysis of GEM in real samples. The results of the effects of various substances that are commonly found in human serum on the interaction of GEM with dsDNA are shown in Fig. 7. The original DPV curves for the selectivity test are given in the supplementary material (Fig. S10). The obtained results showed that the GCE/P(PDCA)/dsDNA electrode was highly selective for GEM-dsDNA interaction.

The stability of the GCE/P(PDCA)/dsDNA electrode was also tested. When the GCE/P(PDCA)/dsDNA electrode was kept in 0.1 mol L^{-1} PBS pH 7.0 at room temperature after voltammetric measurements, the guanine oxidation current signals kept nearly stable in the first 5 days and decreased about 18.4 of its initial response after 20 days, indicating the good stability of the P(PDCA) modified GC electrode.

3.11. Real sample analysis

To investigate the accuracy of the developed method, GCE/P(PDCA)/dsDNA was applied to the analysis of GEM in commercial formulations. For this purpose, the concentration of GEM in the injectable sample was determined. Then certain amounts of GEM were added to the samples and the contents were measured again using the GCE/P(PDCA)/dsDNA by the standard addition method. The results are given in Table 3. The recovery value of the pharmaceutical samples ranged between 97.80% and 99.60%. In the biological sample analysis, standard addition method was used to determine the concentration of GEM and the different amounts of GEM that were spiked into the test sample (Table 4). These results demonstrate the applicability of the proposed electrochemical biosensor based on GCE/P(PDCA)/dsDNA for the determination of GEM in injectable solutions and human serum samples.

4. Conclusion

The proposed electrochemical DNA biosensor is sensitive, selective, and rapid for the determination of GEM at low concentrations. After the interaction of the GEM with the dsDNA, a decrease in guanine and adenine oxidation signals were observed. The GCE/P(PDCA)/dsDNA electrode can not only be used to explore the interaction of GEM with dsDNA, but can also be employed to detect the concentration of GEM. The interaction mechanism between the dsDNA and the GEM was examined by electrochemical, viscosimetric and spectroscopic methods. The results indicated that GEM could change in conformation of the dsDNA, and the binding mode of the GEM to the dsDNA was based on groove binding under these conditions. The proposed biosensor has an excellent applicability for the determination of GEM in human serum samples. Furthermore, the present method could enable the monitoring of new drug compounds for interaction with dsDNA.

Declaration of interest

The authors report no conflicts of interest. The authors are responsible for the content and writing of the paper.

Acknowledgements

This work is produced from Ph.D. thesis of Gözde Aydoğdu Tığ (Ankara University Graduate School of Natural and Applied Sciences) and supported by Ankara University Scientific Research Fund (Grant no. 14L0430004).

Appendix A. Supplementary material

Supplementary data associated with this article can be found in the online version at http://dx.doi.org/10.1016/j.talanta.2016.03.049.

References

[1] M.N. Kirstein, I. Hassan, D.E. Guire, D.R. Weller, J.W. Dagit, J.E. Fisher, R. P. Remmel, High-performance liquid chromatographic method for the determination of gemcitabine and 2′,2′-difluorodeoxyuridine in plasma and tissue culture media, J. Chromatogr. B 835 (2006) 136–142.
[2] R. Rosell, L. Crino, K. Danenberg, G. Scagliotti, G. Bepler, M. Taron, V. Alberola, M. Provencio, C. Camps, F. DeMarinis, J.J. Sanchez, R. Peñas, Targeted therapy in combination with gemcitabine in non-small cell lung cancer, Semin. Oncol. 30 (2003) 19–25.
[3] W. Plunkett, P. Huang, Y.Z. Xu, V. Heinemann, R. Grunewald, V. Gandhi, Gemcitabine: metabolism, mechanisms of action, and self-potentiation, Semin. Oncol. 22 (1995) 3–10.
[4] C. Lanz, M. Früh, W. Thormann, T. Cerny, B.H. Lauterburg, Rapid determination of gemcitabine in plasma and serum using reversed-phase HPLC, J. Sep. Sci. 30 (2007) 1811–1820.
[5] E.R. Wickremsinhe, B.S. Lutzke, B.R. Jones, G.A. Schultz, A.B. Freeman, S.E. Pratt, A.M. Bones, B.L. Ackermann, Quantification of gemcitabine incorporation into human DNA by LC/MS/MS as a surrogate measure for target engagement, Anal. Chem. 82 (2010) 6576–6583.
[6] R. Honeywell, A.C. Laan, C.J. van Groeningen, E. Strocchi, R. Ruiter, G. Giaccone, G.J. Peters, The determination of gemcitabine and 2′-deoxycytidine in human plasma and tissue by APCI tandem mass spectrometry, J. Chromatogr. B 847 (2007) 142–152.
[7] P. Drevenšek, I. Turel, N. Poklar Ulrih, Influence of copper(II) and magnesium (II) ions on the ciprofloxacin binding to DNA, J. Inorg. Biochem. 96 (2003) 407–415.
[8] M.A. Khan, J. Musarrat, Interactions of tetracycline and its derivatives with DNA *in vitro* in presence of metal ions, Int. J. Biol. Macromol. 33 (2003) 49–56.
[9] I.C. Lopes, S.C. Oliveira, A. Oliveira-Brett, In situ electrochemical evaluation of anticancer drug temozolomide and its metabolites–DNA interaction, Anal. Bioanal. Chem. 405 (2013) 3783–3790.
[10] A. Singh, G. Sinsinbar, M. Choudhary, V. Kumar, R. Pasricha, H.N. Verma, S. P. Singh, K. Arora, Graphene oxide-chitosan nanocomposite based electrochemical DNA biosensor for detection of typhoid, Sens. Actuators B Chem. 185 (2013) 675–684.
[11] L. Vergani, G. Mascetti, P. Gavazzo, C. Nicolini, Ethidium bromide intercalation and chromatin structure: a thermal analysis, Thermochim. Acta 294 (1997) 193–204.
[12] Y. Guo, Y. Guo, C. Dong, Ultrasensitive and label-free electrochemical DNA biosensor based on water-soluble electroactive dye azophloxine-functionalized graphene nanosheets, Electrochim. Acta 113 (2013) 69–76.
[13] A.A. Ensafi, E. Heydari-Bafrooei, M. Amini, DNA-functionalized biosensor for riboflavin based electrochemical interaction on pretreated pencil graphite electrode, Biosens. Bioelectron. 31 (2012) 376–381.
[14] A.A. Ensafi, B. Rezaei, M. Amini, E. Heydari-Bafrooei, A novel sensitive DNA–biosensor for detection of a carcinogen, Sudan II, using electrochemically treated pencil graphite electrode by voltammetric methods, Talanta 88 (2012) 244–251.
[15] B. Dogan-Topal, S.A. Ozkan, A novel sensitive electrochemical DNA biosensor for assaying of anticancer drug leuprolide and its adsorptive stripping voltammetric determination, Talanta 83 (2011) 780–788.
[16] A. Abbaspour, M.A. Mehrgardi, Electrocatalytic oxidation of guanine and DNA on a carbon paste electrode modified by cobalt hexacyanoferrate films, Anal. Chem. 76 (2004) 5690–5696.
[17] M. Yousef Elahi, S.Z. Bathaie, S.H. Kazemi, M.F. Mousavi, DNA immobilization on a polypyrrole nanofiber modified electrode and its interaction with salicylic acid/aspirin, Anal. Biochem. 411 (2011) 176–184.
[18] G. Aydoğdu, G. Günendi, D.K. Zeybek, B. Zeybek, Ş. Pekyardımcı, A novel electrochemical DNA biosensor based on poly-(5-amino-2-mercapto-1,3,4-thiadiazole) modified glassy carbon electrode for the determination of nitrofurantoin, Sens. Actuators B: Chem. 197 (2014) 211–219.
[19] F. Berti, S. Todros, D. Lakshmi, M.J. Whitcombe, I. Chianella, M. Ferroni, S. A. Piletsky, A.P.F. Turner, G. Marrazza, Quasi-monodimensional polyaniline nanostructures for enhanced molecularly imprinted polymer-based sensing, Biosens. Bioelectron. 26 (2010) 497–503.
[20] K. Arora, N. Prabhakar, S. Chand, B.D. Malhotra, *Escherichia coli* genosensor based on polyaniline, Anal. Chem. 79 (2007) 6152–6158.
[21] T. Yang, W. Zhang, M. Du, K. Jiao, A PDDA/poly(2,6-pyridinedicarboxylic acid)-CNTs composite film DNA electrochemical sensor and its application for the detection of specific sequences related to PAT gene and NOS gene, Talanta 75 (2008) 987–994.
[22] J. Yang, T. Yang, Y. Feng, K. Jiao, A DNA electrochemical sensor based on nanogold-modified poly-2,6-pyridinedicarboxylic acid film and detection of PAT gene fragment, Anal. Biochem. 365 (2007) 24–30.
[23] L.-L. Li, H. Cai, T.M.-H. Lee, J. Barford, I.M. Hsing, Electrochemical detection of PCR amplicons using electroconductive polymer modified electrode and multiple nanoparticle labels, Electroanalysis 16 (2004) 81–87.
[24] S.S. Kalanur, U. Katrahalli, J. Seetharamappa, Electrochemical studies and spectroscopic investigations on the interaction of an anticancer drug with DNA and their analytical applications, J. Electroanal. Chem. 636 (2009) 93–100.
[25] A. Florea, Z. Guo, C. Cristea, F. Bessueille, F. Vocanson, F. Goutaland, S. Dzyadevych, R. Săndulescu, N. Jaffrezic-Renault, Anticancer drug detection using a highly sensitive molecularly imprinted electrochemical sensor based on an electropolymerized microporous metal organic framework, Talanta 138 (2015) 71–76.
[26] R.M. Buoro, I.C. Lopes, V.C. Diculescu, S.H.P. Serrano, L. Lemos, A.M. Oliveira-Brett, In situ evaluation of gemcitabine–DNA interaction using a DNA-electrochemical biosensor, Bioelectrochemistry 99 (2014) 40–45.
[27] K. Jiao, T. Yang, J. Yang, Y. Feng, Immobilization and hybridization of DNA based on magnesium ion modified 2,6-pyridinedicarboxylic acid polymer and its application for label-free PAT gene fragment detection by electrochemical impedance spectroscopy, Sci. China Ser. B 50 (2007) 538–546.
[28] D.-f. Wang, Z.-h. Wang, T. Zhang, R.-B. Huang, L.-S. Zheng, Novel networks of silver(I) cations assembled with 2,3-pyridinedicarboxylic acid: From 2D sheet to 3D network, J. Mol. Struct. 1068 (2014) 210–215.
[29] B. Ay, N. Doğan, E. Yildiz, İ. Kani, A novel three dimensional samarium(III) coordination polymer with an unprecedented coordination mode of the 2,5-pyridinedicarboxylic acid ligand: hydrothermal synthesis, crystal structure and luminescence property, Polyhedron 88 (2015) 176–181.
[30] M. Karabacak, S. Bilgili, A. Atac, Molecular structure investigation of neutral, dimer and anion forms of 3,4-pyridinedicarboxylic acid: a combined experimental and theoretical study, Spectrochim. Acta Part A Mol. Biomol. Spectrosc. 135 (2015) 270–282.
[31] L. Wang, Z. Wang, E. Wang, Novel hydrogen-bonded three-dimensional network complexes containing copper-pyridine-2,6-dicarboxylic acid, J. Coord. Chem. 57 (2004) 1353–1359.
[32] S.E.-dH. Etaiw, M.M. El-bendary, A new organometallic complex based on the trimethyltin cation and 2,6-pyridinedicarboxylic acid as a potential anticancer agent, Polyhedron 87 (2015) 383–389.
[33] A.T. Çolak, Y. Şahin, O.Z. Yeşilel, F. Çolak, F. Yılmaz, M. Taş, Novel boron compounds of 2,3-and 2,5-pyridinedicarboxylic acids, Inorg. Chim. Acta 383 (2012) 169–177.
[34] L. Wasylina, E. Kucharska, Z. Weglinski, A. Puszko, The13C NMR, UV and IR absorption spectra of pyridinedicarboxylic acids, Chem. Heterocycl. Compd. 35 (1999) 186–194.
[35] A. Nataraj, V. Balachandran, T. Karthick, M. Karabacak, A. Atac, FT-Raman, FT-IR, UV spectra and DFT and *ab initio* calculations on monomeric and dimeric structures of 3,5-pyridinedicarboxylic acid, J. Mol. Struct. 1027 (2012) 1–14.
[36] D. Uzun, A. Balaban Gündüzalp, E. Hasdemir, Selective determination of dopamine in the presence of uric acid and ascorbic acid by N,N′-bis(indole-3-carboxaldimine)-1,2-diaminocyclohexane thin film modified glassy carbon electrode by differential pulse voltammetry, J. Electroanal. Chem. 747 (2015) 68–76.
[37] D.K. Bediako, B. Lassalle-Kaiser, Y. Surendranath, J. Yano, V.K. Yachandra, D. G. Nocera, Structure–activity correlations in a nickel–borate oxygen evolution catalyst, J. Am. Chem. Soc. 134 (2012) 6801–6809.
[38] Z. Yang, M. Xu, Y. Liu, F. He, F. Gao, Y. Su, H. Wei, Y. Zhang, Nitrogen-doped, carbon-rich, highly photoluminescent carbon dots from ammonium citrate, Nanoscale 6 (2014) 1890–1895.
[39] S. Liu, J. Tian, L. Wang, Y. Zhang, X. Qin, Y. Luo, A.M. Asiri, A.O. Al-Youbi, X. Sun, Hydrothermal treatment of grass: a low-cost, green route to nitrogen-doped, carbon-rich, photoluminescent polymer nanodots as an effective fluorescent sensing platform for label-free detection of Cu(II) ions, Adv. Mater. 24 (2012) 2037–2041.
[40] A.A. Ensafi, E. Heydari-Bafrooei, B. Rezaei, Different interaction of codeine and morphine with DNA: a concept for simultaneous determination, Biosens. Bioelectron. 41 (2013) 627–633.
[41] A. Erdem, B. Kosmider, R. Osiecka, E. Zyner, J. Ochocki, M. Ozsoz, Electrochemical genosensing of the interaction between the potential chemotherapeutic agent, cis-bis(3-aminoflavone)dichloroplatinum(II) and DNA in comparison with cis-DDP, J. Pharm. Biomed. Anal. 38 (2005) 645–652.
[42] B. Dogan-Topal, B. Uslu, S.A. Ozkan, Voltammetric studies on the HIV-1 inhibitory drug Efavirenz: the interaction between dsDNA and drug using

electrochemical DNA biosensor and adsorptive stripping voltammetric determination on disposable pencil graphite electrode, Biosens. Bioelectron. 24 (2009) 2358–2364.
[43] M.T. Carter, M. Rodriguez, A.J. Bard, Voltammetric studies of the interaction of metal chelates with DNA. 2. Tris-chelated complexes of cobalt(III) and iron(II) with 1,10-phenanthroline and 2,2′-bipyridine, J. Am. Chem. Soc. 111 (1989) 8901–8911.
[44] K.M. Naik, S.T. Nandibewoor, Electro-oxidation and determination of gemcitabine hydrochloride, an anticancer drug at gold electrode, J. Ind. Eng. Chem. 19 (2013) 1933–1938.
[45] N.L. Teradal, S.S. Kalanur, S.N. Prashanth, J. Seetharamappa, Electrochemical investigations of an anticancer drug in the presence of sodium dodecyl sulfate as an enhancing agent at carbon paste electrode, J. Appl. Electrochem. 42 (2012) 917–923.
[46] K.E. Erkkila, D.T. Odom, J.K. Barton, Recognition and reaction of metallointercalators with DNA, Chem. Rev. 99 (1999) 2777–2795.
[47] H. Nawaz, S. Rauf, K. Akhtar, A.M. Khalid, Electrochemical DNA biosensor for the study of ciprofloxacin–DNA interaction, Anal. Biochem. 354 (2006) 28–34.
[48] B. Rafique, A.M. Khalid, K. Akhtar, A. Jabbar, Interaction of anticancer drug methotrexate with DNA analyzed by electrochemical and spectroscopic methods, Biosens. Bioelectron. 44 (2013) 21–26.
[49] Y.-J. Guo, J.-B. Chao, J.-H. Pan, Study on the interaction of 5-pyridine-10,15,20-tris-((*p*-chlorophenyl))porphyrin with cyclodextrins and DNA by spectroscopy, Spectrochim. Acta Part A Mol. Biomol. Spectrosc. 68 (2007) 231–236.
[50] S.U. Rehman, T. Sarwar, M.A. Husain, H.M. Ishqi, M. Tabish, Studying non-covalent drug–DNA interactions, Arch. Biochem. Biophys. 576 (2015) 49–60.
[51] J.-H. Shi, J. Chen, J. Wang, Y.-Y. Zhu, Binding interaction between sorafenib and calf thymus DNA: spectroscopic methodology, viscosity measurement and molecular docking, Spectrochim. Acta Part A Mol. Biomol. Spectrosc. 136 (Part B) (2015) 443–450.
[52] J. Xie, D. Chen, Q. Wu, J. Wang, H. Qiao, Spectroscopic analyses on interaction of melamine, cyanuric acid and uric acid with DNA, Spectrochim. Acta Part A Mol. Biomol. Spectrosc. 149 (2015) 714–721.
[53] S. Mahadevan, M. Palaniandavar, Spectroscopic and voltammetric studies on copper complexes of 2,9-dimethyl-1,10-phenanthrolines bound to calf thymus DNA, Inorg. Chem. 37 (1998) 693–700.
[54] L. Strekowski, B. Wilson, Noncovalent interactions with with DNA: an overview, Mutat. Res./Fundam. Mol. Mech. Mutagen. 623 (2007) 3–13.